

Polar fluctuations and first-order Raman scattering in highly polarizable KTaO_3 crystals with off-center Li and Nb ions

P. DiAntonio, B. E. Vugmeister, and J. Toulouse

Physics Department, Lehigh University, Bethlehem, Pennsylvania 18015

L. A. Boatner

Oak Ridge National Laboratory, Oak Ridge, Tennessee 37831

(Received 31 July 1992)

Relatively low concentrations of randomly substituted off-center ions are known to induce ferroelectric order in highly polarizable crystals. In the case of potassium tantalate (KTaO_3) doped with lithium or niobium, the results of first-order Raman scattering from two hard phonon modes (TO_2 and TO_3) show that polar microregions are formed at relatively high temperatures. At lower temperatures, and above a certain critical dopant concentration, the Raman results are consistent with the occurrence of a structural phase transition. These results can be reasonably explained by using a random-molecular-field theory that takes into account the indirect dipolar interactions mediated by the soft lattice. This approach accounts for the characteristic asymmetry of the TO_2 Raman scattering detected at high temperatures and for the subsequent increase in the integrated scattering intensity with decreasing temperature. An analysis of the Raman results provides a means for determining the size of the polar microregions formed in the highly polarizable KTaO_3 lattice. The good agreement obtained between the theoretical and experimental results provides support to the physical concepts embodied in the present theoretical approach to describing the onset of order in these systems.

INTRODUCTION

Highly polarizable crystal lattices doped with ions that can occupy off-center positions offer particularly interesting opportunities for the study of collective effects associated with impurities in condensed matter. These collective effects can include impurity-induced fluctuations and phase transitions as well as disorder and other effects. During the past 15 years, the study of highly polarizable crystalline materials such as KTaO_3 doped with off-center impurities has led to the observation of new types of interactions and effects. Recently, the results of these previous studies have been summarized and reviewed.^{1,2} In spite of these relatively extensive prior investigations, the physical nature of the effects observed in systems of this type is still a subject of considerable controversy, and the experimental results have only provided partial answers to fundamental questions such as the following: (1) Does the system undergo a normal ferroelectric transition at low dopant concentrations or is some type of dipolar glass state formed? (2) What factors determine the critical concentration for the occurrence of a ferroelectric transition? (3) How does the physical nature of the transition evolve with increasing dopant concentration?

While pure KTaO_3 exhibits a soft mode that is associated with a relatively high dielectric permittivity (up to ~ 5000), the material, in fact, remains in the paraelectric state down to the lowest temperatures. This type of behavior has been denoted as "incipient ferroelectricity." When KTaO_3 is doped with a sufficient concentration of Li impurities ([100] off-center substituted for K) or Nb impurities ([111] off-center substituted for Ta), structural

and ferroelectric transitions are induced whose characteristics vary with the amount of dopant incorporated in the KTaO_3 host. Relatively recent experimental evidence indicates that, in $\text{K}_{1-x}\text{Li}_x\text{TaO}_3$ (KLT) and $\text{KTa}_{1-x}\text{Nb}_x\text{O}_3$ (KTN), this transition can occur for impurity concentrations as low as $x_{\text{Li}} \sim 2\%$ for Li and $x_{\text{Nb}} \sim 1.2\%$.^{3,4}

It is important to note that the characteristics of the phase transitions in these impurity systems are significantly different from those taking place in conventional undoped ferroelectric materials. In particular, for both KLT and KTN the size of the domains having an approximately homogeneous spontaneous polarization is apparently significantly smaller than the size of the structural domains (see, for example, the discussion and references in Ref. 5). Nevertheless, the coincidence of the temperature of the maximum of the dielectric permittivity with the appearance of other anomalies that are characteristic of a structural transformation is an unambiguous sign of a ferroelectric-type of phase transition.

The cases of off-center Li and Nb impurities in KTaO_3 represent examples of slowly relaxing defects of the type described in the work of Halperin and Varma,⁶ since at sufficiently low temperatures the frequencies of the reorientational jumps of such impurities between different off-center sites are less than the soft-mode frequency of pure KTaO_3 . As shown in Ref. 7, polar lattice distortions induced by such slowly relaxing impurities in highly polarizable crystals can be represented as a sum of the usual anisotropic dipolar terms plus a new isotropic term resulting from the strong spatial dispersion of the dielectric permittivity. This spatial dispersion is, in fact, very

significant for the case of highly polarizable crystals.

Since Raman scattering is a "local" probe, it is an experimental technique that is well suited to the investigation of the nature of isotropic distortions in a crystal lattice on an atomic scale. In fact, as pointed out early on by Yacoby,⁸ in the case of isotropic distortions which extend over a few lattice constants in a crystal, the selection rules for Raman scattering can be altered in such a way that first-order scattering can be observed even in the nominally high-symmetry cubic phase of the material. This point has been investigated further by Uwe *et al.*,⁹ and, additionally, Bruce, Taylor, and Murray¹⁰ have argued that such an apparent violation of the selection rules apparently takes place near all phase transitions that exhibit precursor effects. In general, however, one would expect that the observation of first-order scattering in the high-symmetry phase would depend on the specific nature of these precursor effects. In particular, in the present case of KTaO_3 , the Raman scattering strongly depends on the type of impurity and on the impurity concentration.

First-order Raman scattering (FORS) in KTN was initially reported by Yacoby⁸ who attributed the observed effects to Nb-induced fluctuations. This interpretation was challenged by Prater, Chase, and Boatner¹¹ and by Uwe *et al.*,⁹ based on the lack of a simple relationship between the intensity of the Raman spectra and the Nb concentration. Alternatively, these workers suggested that the Nb simply induced a ferroelectric phase transition and that the observed FORS was due to the presence of other unknown impurities. This alternative point of view was further supported by the fact that FORS was also observed in some nominally pure KTaO_3 crystals and by the observation that the first-order features appeared to differ in KLT and KTN.

The two purposes of the present work are, to contribute to a resolution of the controversy surrounding the problem of first-order Raman scattering that is observed in highly polarizable crystals doped with off-center ions, and to provide new insight into the nature of the transitions observed for the KLT and KTN systems. To that effect, we have carried out a detailed investigation of the Raman spectra of two of the hard modes, TO_2 and TO_3 , observed in KLT and KTN crystals. These hard modes are characterized by very narrow linewidths relative to the soft TO_1 mode investigated previously in Ref. 9, and accordingly, detailed comparisons between the experimental and theoretical results can be made.

EXPERIMENTAL RESULTS

As established by the results of previous studies, four distinct transverse-optic modes, labeled TO_1 , TO_2 , TO_3 , and TO_4 , are observed for KTN, KLT, and KTaO_3 .¹² All four of these modes have odd parity and, therefore, should not be Raman active in the paraelectric cubic phase. Nevertheless, the three polar modes (the soft TO_1 mode and the TO_2 and TO_4 modes) are clearly observed above the paraelectric-to-ferroelectric transition temperature T_c in all KLT and KTN crystals.⁴

In the present work, precise measurements have been

made of the Raman spectra corresponding to the hard TO_2 and TO_3 modes for $\text{K}_{1-x}\text{Li}_x\text{TaO}_3$ ($x = 1\%$, 4% , and 10%) and in $\text{KTa}_{1-x}\text{Nb}_x\text{O}_3$ ($x = 1.2\%$, 4% , and 15.7%). The single crystals employed in these investigations were grown from a nonstoichiometric melt using a process described previously. The KTN 1.2% Nb crystal was provided by D. Rytz of Sandoz Products in Basel, Switzerland. The Raman-scattering measurements were carried out using a U-1000 ISA spectrometer with a double monochromator and the 488-nm line of an argon laser. The single-crystal specimens were equilibrated for 15 min at each temperature before the spectral data were collected.

Figure 1 illustrates typical examples of the Raman-scattering spectra obtained for both KLT and KTN crystals. All of these spectra were characterized by a strongly asymmetric character observed for the TO_2 line, which is otherwise relatively narrow ($\Delta\omega_{\text{HM}} \sim 2\text{--}3\text{ cm}^{-1}$). Additionally, as can be seen from the spectra shown in Fig. 1, both the linewidth and asymmetry increase with dopant concentration and are greater for the Li-doped than for the Nb-doped crystals. In contrast to the asymmetry exhibited by the TO_2 line, the TO_3 line, as can be seen in Fig. 2, is highly symmetric.

The temperature dependence of the integrated intensity I_N of the TO_2 line is shown in Fig. 3 along with the linewidth $\Delta\omega_{\text{HM}}$. The temperature dependence of I_N is apparently similar for all of the crystals investigated, except for the case of the 1% KLT sample where no TO_3 mode was observed in agreement with the expected absence of a transition for low concentrations. For the other samples, however, it is possible to observe the TO_2 scattering at a relatively high temperature above T_c —this is particularly true for the case of the Li-doped samples. As the temperature is lowered, I_N increases to a maximum value and then decreases at T_c . The intensity subsequently increases as the temperature is further decreased. As has recently been demonstrated,⁴ the decrease in intensity of the TO_2 line at T_c is accompanied by the appearance of a narrow, symmetrical TO_3 line in

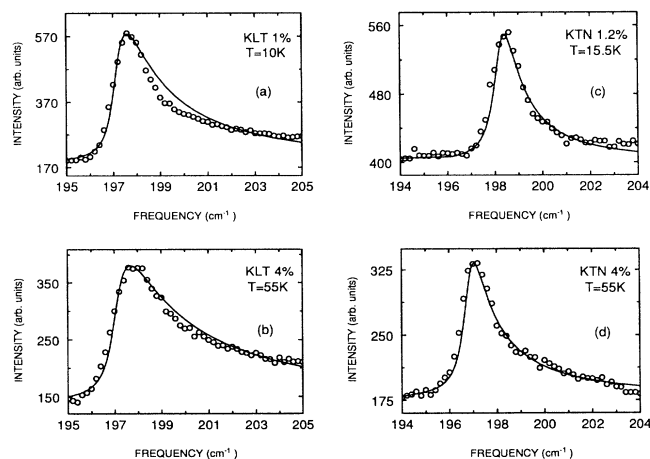


FIG. 1. TO_2 Raman spectra for (a), (b) KLT and (c), (d) KTN samples. Solid lines represent the fit obtained by using Eq. (19).

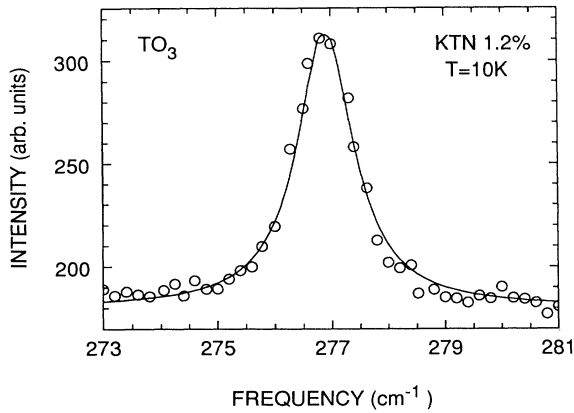


FIG. 2. Typical shape of the TO_3 Raman lines. The solid curve is the fit with a Lorentzian line shape.

the Raman spectra which corresponds to the occurrence of the structural ferroelectric phase transition. It should be noted that the results for the 4% Nb sample are somewhat unusual in that, while they do not exhibit a very pronounced maximum and subsequent drop of I_N , the material otherwise behaves normally.

Finally, it is worthwhile to reemphasize the two major differences between the Li- and Nb-doped $KTaO_3$ crystals. First, in the case of KLT, the TO_2 line can be observed at temperatures as much as 200 K above T_c , and its integrated intensity I_N increases more slowly with decreasing temperature. The TO_2 line in KTN, on the other hand, appears closer to T_c and I_N increases more rapidly to the maximum value exhibiting a stronger temperature dependence than that characteristic of the KLT samples. Second, both the width and asymmetry of the TO_2 line are greater for KLT than for KTN. In the case of the 1% Li-doped KLT sample, the linewidth decreases monotonically, reaching a minimum at the lowest temperatures. For the other specimens, the TO_2 linewidth decreases relatively abruptly upon going through the

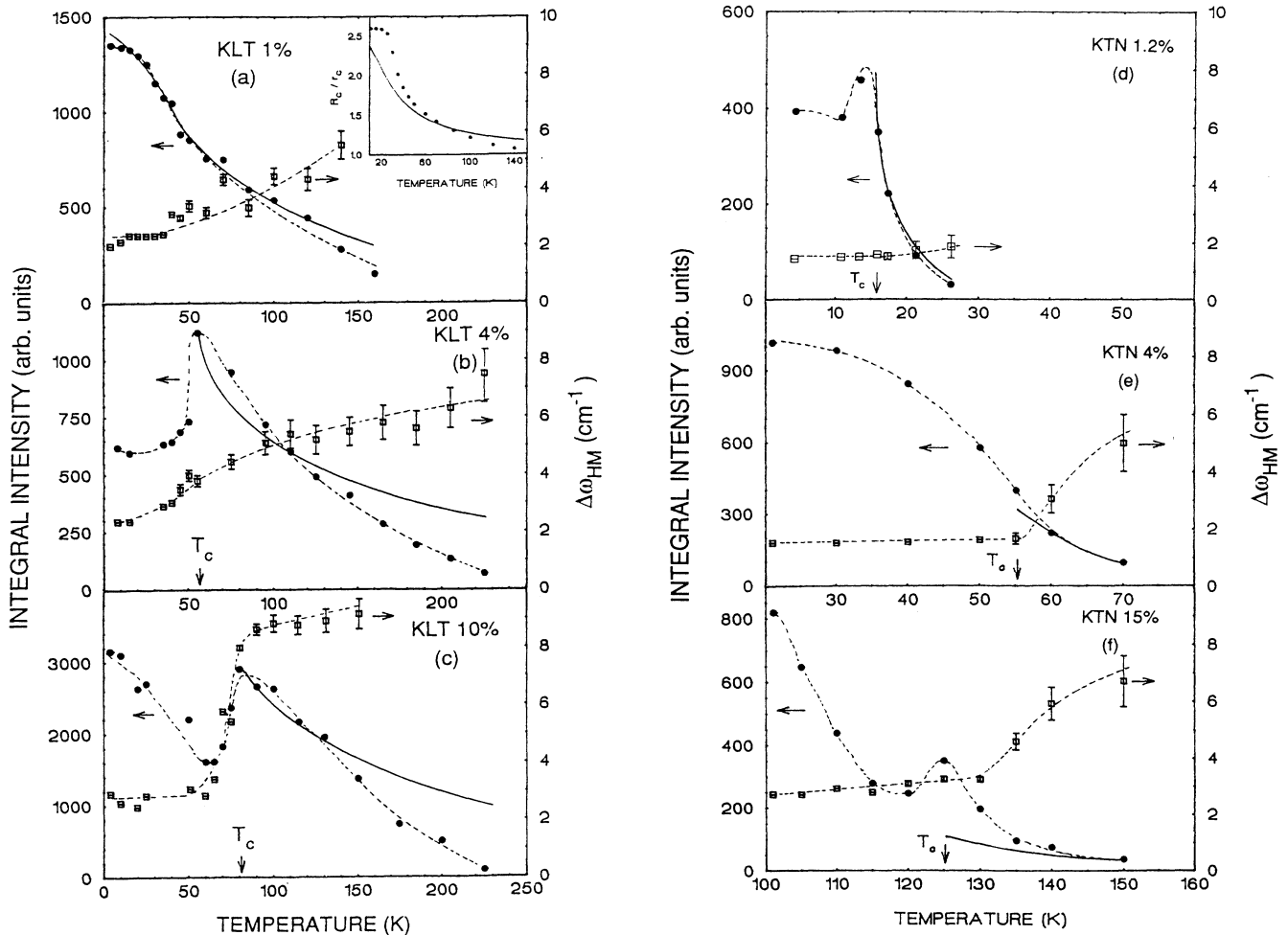


FIG. 3. Integrated intensities I^h for (a)–(c) KLT and (d)–(f) KTN samples. Solid lines show the fit obtained with Eq. (18) for KLT and Eq. (34) for KTN. Indicated T_c 's correspond to the observation of a sharp TO_3 line in the spectrum.

phase transition where the degree of decrease becomes greater with increasing dopant concentration.

THEORY

Changes induced in the electronic polarizability $\alpha(r, t)$, due to polar optic phonons, can be written in the form

$$\delta\alpha(r, t) = \mathbf{P}(r, t) \cdot \hat{\Lambda} \cdot \mathbf{P}(r, t), \quad (1)$$

where $P(r, t)$ represents the space- and time-dependent polarization fluctuations and $\hat{\Lambda}$ is a fourth-rank tensor. Equation (1) usually describes second-order Raman scattering. However, if the polarization-fluctuation spec-

trum contains a low-frequency component such as slow-relaxational polar modes induced by off-center ions, Eq. (1) can describe single-phonon Raman scattering as well. To illustrate this, we write the polarization as a sum over the components due to the polar hard modes P^h and the slow-relaxing component P^μ :

$$P = \sum_h P^h + P^\mu. \quad (2)$$

In order to explain the appearance of a single-phonon Raman line above T_c , we are only concerned in Eq. (1) with the cross terms $P^\mu P^h$ ($P^h = P^{\text{TO}_2}$ specifically). The scattering intensity can be written in the form

$$\begin{aligned} I^h(\omega) &\sim \langle \delta\alpha(r, t) \delta\alpha(0, 0) \rangle_{q \approx 0, \omega} \\ &\sim \sum_q \int d\omega' \langle P^\mu(r, t) P^\mu(0, 0) \rangle_{q'\omega'} \langle P^h(r, t) P^h(0, 0) \rangle_{-q', \omega - \omega'}. \end{aligned} \quad (3)$$

Here the bracketed terms in Eq. (3) include both thermal averaging and averaging over random-dipole configurations. For the Stokes component of the scattered light, one can write

$$\langle P^h(r, t) P^h(0, 0) \rangle_{q, \omega} \sim \frac{1}{\Omega_q} \frac{\Gamma}{\Gamma^2 + (\omega - \Omega_q)^2}, \quad (4)$$

where we have omitted the phonon-occupancy numbers $n(\Omega_q)$ for temperatures $kT < \hbar\Omega_q$. We also describe the phonon spectral density by a simple Lorentz form that should be valid for frequencies ω close to the hard phonon frequency Ω_q , as is the case for the Raman results reported here.

To describe the slow-relaxing polarization $\mathbf{P}^\mu(\mathbf{r}, t)$ induced by off-center ions, we utilize the model that was suggested in Ref. 7. According to this model, which is valid when the reorientational frequency of the off-center ions ν is less than the soft-mode frequency ω_s of pure KTaO_3 , we can obtain the polarization $P^\mu(r, t)$ from the static Hamiltonian¹³

$$H = \frac{2\pi}{\epsilon_0} V_0 \sum_{qs} (1 + r_c^2 q^2) P_{qs} P_{-qs} - \frac{4\pi}{3} \gamma \sum_i \mathbf{d}_i \cdot \mathbf{P}(r_i). \quad (5)$$

Here P_{qs} is the \mathbf{q} Fourier component of the polarization $\mathbf{P}(\mathbf{r})$ arising from the soft mode of pure KTaO_3 and s designates either one of the two transverse branches of this mode; ϵ_0 and r_c are, respectively, the dielectric permittivity and the correlation length of the polarization in the pure lattice, and V_0 is the crystal volume. In the long-wavelength and linear approximations, the second term in Eq. (5) is responsible for the interaction between the host-lattice polarization and the dipole moment d_i of the off-center ions, and γ is the parameter describing the strength of this interaction.

Because the polarization fluctuations induced by the impurity dipoles are low-frequency ones ($\nu \ll \omega_s$), they can be assumed to satisfy the adiabatic approximation and to follow the instantaneous values of the dipoles. Accordingly, they can be determined from a minimization of the Hamiltonian of Eq. (5) with respect to P_{qs} . Setting

$(\partial H / \partial P_{qs}) = 0$, we find that the polarization induced by the dipoles is given by

$$P_\alpha^\mu(\mathbf{r}_i) = \frac{\epsilon_0}{4\pi} \sum_{j\beta} K_{ij}^{\alpha\beta}(\mathbf{r}_{ij}) d_{j\beta}^*, \quad (6)$$

where $d_j^* = \gamma \epsilon_0 d_j / 3$ is the effective dipole moment of the impurity in the highly polarizable crystal. The Fourier components $\hat{\mathbf{K}}_q$ of the matrix $\hat{\mathbf{K}}(r)$ are given by the expression¹³

$$K_q^{\alpha\beta} = \frac{4\pi}{\epsilon_0 V_0 (1 + r_c^2 q^2)} \left[\delta_{\alpha\beta} - \frac{q_\alpha q_\beta}{q^2} \right], \quad (7)$$

where $\delta_{\alpha\beta}$ is the Kronecker delta symbol with $\alpha, \beta = x, y, z$.

Using Eq. (6), we can write the correlation function $\langle P^\mu(r, t) P^\mu(0, 0) \rangle_{q\omega}$ at temperatures $T \gtrsim T_c$ in the form

$$\langle P^\mu(r, t) P^\mu(0, 0) \rangle_{q\omega} = K_q S_{q\omega} K_{-q}, \quad (8)$$

where $S_{q\omega}$ is the dynamic structure factor describing correlations between the orientations of different dipoles:

$$S_{q\omega} = N \langle d_i^*(t) d_i^* \rangle_\omega + N^2 \langle d_i^*(t) d_j^* \rangle_{q\omega}. \quad (9)$$

The quantity $S_{q\omega}$, as determined from the fluctuation-dissipation theorem, is

$$S_{q\omega} = \frac{2K_B T}{\omega} \chi''_{q\omega}. \quad (10)$$

The Hamiltonian describing the interactions of dipoles in the highly polarizable crystal, as follows from Eqs. (6) and (7), can be written in the form

$$V_{dd} = -\frac{1}{2} \sum_{ij} \mathbf{d}_i^* \cdot \hat{\mathbf{K}}_{ij} \cdot \mathbf{d}_j^*. \quad (11)$$

Therefore, in the random-phase approximation, we have the result¹³

$$\langle P^\mu(r, t) P^\mu(0, 0) \rangle_{q\omega} = \langle P^\mu(r) P^\mu(0) \rangle_q \frac{\nu_q}{\nu_q^2 + \omega^2}, \quad (12)$$

where ν_q is the relaxation frequency of the q th Fourier component of the fluctuations, which determines the width of the central peak.

In the following treatment, we designate the critical correlation length by R_c , which in the doped crystal diverges at the impurity-induced ferroelectric phase transition:

$$R_c^2 = \frac{\epsilon}{\epsilon_0} r_c^2, \quad (13)$$

where ϵ is the dielectric permittivity of the doped crystal. Now ν_q can be expressed as

$$\nu_q = \nu \frac{R_c^{-2} + q^2}{r_c^{-2} + q^2}. \quad (14)$$

In Eq. (12) the static part of the fluctuation of polarization induced by off-center ions is equal to¹³

$$\langle P^\mu(r) P^\mu(0) \rangle_q \sim \frac{1}{(R_c^{-2} + q^2)(r_c^{-2} + q^2)}, \quad T \gtrsim T_c. \quad (15)$$

Equation (15) represents, for a given q , the integrated intensity of the low-frequency fluctuation spectra of polarization.

One can compare this low-frequency part with the full static spectrum of the polarization fluctuations for crystals containing off-center ions. Following a treatment similar to that employed in Ref. 6, from Eq. (5) we obtain the result

$$\langle P(r) P(0) \rangle_q \sim \frac{1}{(R_c^{-2} + q^2)}. \quad (16)$$

The major difference between Eqs. (15) and (16) is the additional factor of $(r_c^{-2} + q^2)^{-1}$ in Eq. (15). Because of this factor, short-wavelength fluctuations with $q > r_c^{-1}$ are spontaneously cut off and the fluctuation spectrum is "smoothed" out, since r_c is several times the lattice constant in soft lattices. As a result of this spontaneous cutoff, one can calculate the mean-square polarization fluctuations directly by summing Eq. (15) over all q 's without imposing an arbitrary limit:

$$\langle (P^\mu)^2 \rangle = \sum_q \langle P^\mu(r) P^\mu(0) \rangle_q. \quad (17)$$

Using Eq. (15) in Eq. (17), we find

$$\langle (P^\mu)^2 \rangle \sim \frac{r_c}{1 + r_c/R_c}. \quad (18)$$

We emphasize that, in highly polarizable crystals, only by taking the exact expression for the static spectrum Eq. (15) and not Eq. (16) can one obtain the correct value of $\langle (P^\mu)^2 \rangle$ directly from Eq. (17). This was not appreciated in Refs. 8 and 14, where an equation similar to Eq. (16) was used and the summation was arbitrarily cut off at $q_{\max} \sim R_c^{-1}$. Equations (13) and (15) clearly show that, in highly polarizable crystals, q_{\max} has to be of the order $r_c^{-1} > R_c^{-1}$.

We note that, even though the Hamiltonian in Eq. (5)

was written in the harmonic approximation, it was shown in Ref. 15 that the effects of anharmonicity can be approximately included in Eq. (5) through a renormalization of the parameter r_c which can depend on the concentration of off-center ions.

Combining Eqs. (4), (12), and (15) into Eq. (3), we find that the Raman scattering associated with the polar hard modes is the product of two contributions: the dynamic homogeneous broadening $g(\omega, \omega')$ connected with the finite lifetime of the hard mode and the dipole reorientation time, on the one hand, and the static inhomogeneous broadening $\varphi(\omega')$ caused by the joint effects of polarization fluctuations and the dispersion of the hard mode on the other. The following result is then obtained:

$$I^h(\omega) \sim \int d\omega' \varphi(\omega') g(\omega, \omega'), \quad (19)$$

where

$$g(\omega, \omega') = \frac{(\nu(\omega') + \Gamma)}{(\nu(\omega') + \Gamma)^2 + (\omega - \omega')^2} \quad (20)$$

represents the dynamic homogeneous part and

$$\varphi(\omega) = \int \frac{q^2 dq}{(r_c^{-2} + q^2)(R_c^{-2} + q^2)} \frac{1}{\Omega_q} \delta(\omega - \Omega_q) \quad (21)$$

is the static inhomogeneous contribution. In Eq. (20), $\nu(\omega') = \nu(q_{\omega'})$, where $q_{\omega'}$ is obtained from the dispersion relation: $\omega' = \Omega_{q_{\omega'}}$.

In the present analysis, we have assumed a quadratic dependence of Ω_q on q :

$$\Omega_q^2 = \Omega_0^2 + v_h^2 q^2, \quad (22)$$

where Ω_0 is the hard-mode frequency at $q=0$ and v_h is a phase velocity.

For $\omega - \Omega_0 \ll \Omega_0$, we have, from Eqs. (21) and (22),

$$\varphi(\omega) = \begin{cases} \frac{\sqrt{\omega - \Omega_0}}{(\omega - \Omega_0 + r_c^{-2} v_h^2 / 2\Omega_0)(\omega - \Omega_0 + R_c^{-2} v_h^2 / 2\Omega_0)}, & \omega \geq \Omega_0, \\ 0, & \omega < \Omega_0. \end{cases} \quad (23)$$

Two opposite limits can be considered for $I^h(\omega)$, depending on the ratio between $\nu + \Gamma$ and the quantity $r_c^{-2} v_h^2 / 2\Omega_0$.

(i) $\nu + \Gamma \gg r_c^{-2} v_h^2 / 2\Omega_0$; i.e., the function $g(\omega, \omega')$ is much broader than the function $\varphi(\omega')$. In this "dynamic" limit, it follows from Eqs. (19) and (15) that

$$I^h(\omega) \sim g(\omega, \Omega_0) \int \varphi(\omega') d\omega' \sim g(\omega, \Omega_0) \langle (P^\mu)^2 \rangle. \quad (24)$$

Therefore, in this dynamic limit, the intensity of the hard-mode Raman line is proportional to the mean-square fluctuation $\langle (P^\mu)^2 \rangle$ of the order parameter, which can be considered as a measure of the precursor order.¹⁰ The shape of the line coincides with the shape of $g(\omega)$, which, in the general case, can be more complicated than the simple Lorentz form used in (20). This limit was considered in Refs. 8 and 10.

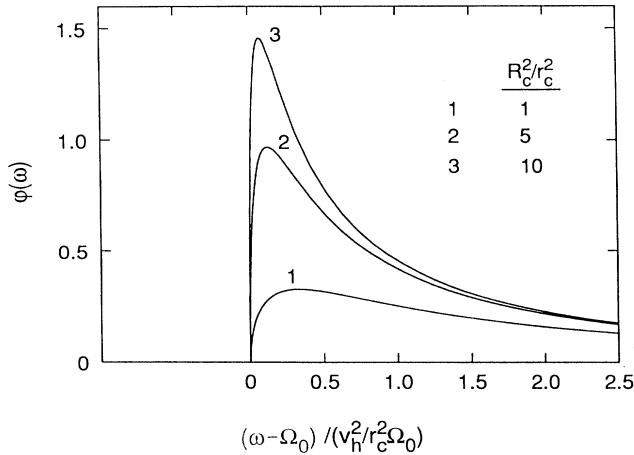


FIG. 4. Shape of the function $\varphi(\omega)$, Eq. (23), for different values of R_c/r_c .

(ii) $\nu + \Gamma \ll r_c^{-2}v_h^2/2\Omega_0$. In this static limit, one can replace $g(\omega, \omega')$ by the delta function $\delta(\omega - \omega')$, leading to

$$I^h(\omega) \sim \varphi(\omega). \quad (25)$$

The function $\varphi(\omega)$ is illustrated in Fig. 4 for different values of the ratio R_c/r_c . The line is very asymmetrical with the high-frequency portion slowly decreasing as $(\omega - \Omega_0)^{-3/2}$.

It should also be noted that, according to Eqs. (19)–(21), the integral intensity of the line $\int I^h(\omega) d\omega \sim \langle (P^\mu)^2 \rangle$ is independent of the ratio between $\nu + \Gamma$ and $r_c^{-2}v_h^2/2\Omega_0$.

ANALYSIS OF THE KLT SPECTRA

In the following treatment, we analyze the shape of the experimental KLT spectra and the integral intensity of the TO_2 line. As noted in the experimental results section, the characteristic feature of the TO_2 line is its asymmetry when compared to the symmetric Lorentzian TO_3 line. We also note that the hard phonon damping contribution to the linewidth 2Γ must not be very different for the TO_2 and TO_3 modes since their widths at half maximum are of the same order of magnitude, i.e., $\Delta\omega_{\text{HM}}^{\text{TO}_2} \approx \Delta\omega_{\text{HM}}^{\text{TO}_3}$. We therefore conclude that the essential difference between the shapes of the two lines is due to the extra contribution of the inhomogeneous broadening $\varphi(\omega)$ to the TO_2 line shape. Nevertheless, because the

width $\Delta\omega_{\text{HM}}^{\text{TO}_2}$ is of the same order as $\Delta\omega_{\text{HM}}^{\text{TO}_3} = 2\Gamma^{\text{TO}_3}$, we must use the general formulas given in Eqs. (19)–(21) in order to extract accurate values for the parameters Γ^{TO_2} and $r_c^{-2}v_h^2/2\Omega_0$. One simplification is, however, possible in Eq. (20), since it is well known that the reorientational frequency of the off-center Li ion follows an Arrhenius law $\nu = \nu_0 \exp(-U/T)$ with $\nu_0 = 1.6 \times 10^{13} \text{ s}^{-1}$ and $U \approx 1000 \text{ K}$.¹⁶ This law yields $\nu < 1.5 \text{ cm}^{-1}$ (i.e., less than the experimental TO_2 linewidth) for $T < 170 \text{ K}$. Consequently, in the temperature region of interest, we have treated Li ions as static impurities and have neglected ν in Eq. (20). Theoretical fits of Eqs. (19)–(21) to the experimental line shapes for different Li concentrations are presented in Fig. 1 as solid lines. The values obtained for the pertinent parameters are given in Table I. The damping contribution to the linewidth of the TO_2 mode, $\Gamma^{\text{TO}_2} \approx 0.4 \text{ cm}^{-1}$, is found to be close to that of the TO_3 mode, $\Gamma^{\text{TO}_3} \approx 0.7 \text{ cm}^{-1}$. The values of the ratio R_c/r_c are also found to increase with the Li concentration. Below T_c the temperature-independent shape of the TO_2 line implies that R_c is a constant, in agreement with the second-harmonic generation results of Azzini *et al.*⁵ With this latter technique, however, they were not able to determine R_c above the transition as permitted by Raman scattering.

The integral intensities I_N and linewidths are presented in Fig. 3. The temperature dependence of I_N is seen to be stronger for higher concentrations. Above T_c , this is primarily due to the more rapid increase of R_c which follows the $\epsilon(T)$ dependence as indicated in Eq. (13). We also note that the values of R_c/r_c obtained from fitting the Raman spectra are very close to a Curie-Weiss law [$R_c^2/r_c^2 \sim (1 - T_c/T)^{-1}$]. The solid lines in Fig. 3 represent fits of Eq. (18) to the experimental I_N data, using the ratio R_c/r_c previously obtained from the experimental spectra. While the overall temperature dependence is reproduced, its specific functional form is not, the discrepancy being stronger the higher the concentration. This effect most likely arises from the initial assumption that Li can be regarded as a static impurity. The limited validity of this assumption is suggested by the linewidth, which is observed to decrease at the phase transition.

The 1% Li sample offers an unexpected result. Despite the accepted fact that there is no ferroelectric phase transition for this Li concentration,^{1,2} our fitting results Fig. 3(a) show that the correlation length R_c is still approximately 2.5 times as long as r_c at low temperatures. This

TABLE I. Values of the parameters R_c/r_c and v_h/r_c obtained by fitting Eqs. (19)–(21) to the experimental line shapes. The corresponding experimentally determined values of ϵ/ϵ_0 and ω_s are included for comparison.

	T	R_c/r_c	$(\epsilon/\epsilon_0)_{\text{expt}}^{1/2}$	v_h/r_c	$(\omega_s)_{\text{expt}}$
KLT 1%	10	2.5	< 1	35	43
KLT 4%	55	4.5	2	49	67
KLT 10%	80	6.3		69	71
KTN 1.2%	15.5	4.6	5	17	16
KTN 4%	55	6.8		33	
KTN 15.7%	125	11.8	12	53	58

finding might explain recent ultrasonic results that show an anomaly in the sound velocity in the same crystal, suggestive of a local phase transition.¹⁷ This experimental finding is also close to the results of Azzini *et al.*,⁵ who obtained $R_c \approx 50 \text{ \AA}$ or $R_c/r_c \approx 2.5$ for $x = 1.6$.

The increase of R_c with decreasing temperature can be reproduced qualitatively by the model presented above with a previously developed random-molecular-field approximation^{18,19} that takes into account the fluctuations of the local fields acting on every Li dipole.

We have performed the present calculation for an eight-orientation dipole system, but it is clear that the general applicability of the model should not be affected by the fact that the present KLT system is only a six-orientation dipole system. As estimated in Ref. 19, for $x \geq 1\%$ one can neglect the effect of fluctuations of the dipolar field induced by the Li dipoles on their own ordering. The static random fields already present in pure KTaO_3 (Ref. 9) nevertheless constitute an additional source of fluctuation of the local fields. Because of such static random fields, a ferroelectric phase transition does not take place below a critical concentration $x_{cr} \approx 2\%$.³ According to Ref. 19 and taking into account fluctuations of the local field, we find

$$\frac{r_c^2}{R_c^2} = 1 - \frac{1}{\sqrt{3}} \int_{-\infty}^{\infty} dE \tanh \left[\frac{E}{K_B T \sqrt{3}} \right] \left. \frac{\partial f(E, L)}{\partial L} \right|_{L=0}, \quad (26)$$

where $L = \langle d \rangle / d$ is the long-range order parameter and $f(E, L)$ is the distribution function of the local fields. We have performed explicit calculations of Eq. (26), assuming a Gaussian form for $f(E, L)$, i.e.,

$$f(E, L) = \frac{1}{\sqrt{2\sigma}} \exp \left[-\frac{(E - E_0 L)^2}{2\sigma^2} \right], \quad (27)$$

where $E_0 = (d^*)^2 \sum_{j\beta} \langle K_{ij}^{\alpha\beta} \rangle$ is a linear function of the Li concentration and σ is the second moment of the static random-field distribution. In the case of a very narrow random-field distribution (i.e., where $\sigma \ll E_0$), $f(E, L)$ can be approximated by a delta function $f(E, L) = \delta(E - E_0 L)$, leading to a mean-field Curie-Weiss dependence ($r_c^2/R_c^2 = 1 - T_c^{\text{MF}}/T$) with a transition temperature $T_c^{\text{MF}} = E_0/3$. Near and below the critical concentration, however, the opposite limit $E_0 \lesssim \sigma$ is applicable, leading to a significant change in the temperature dependence of the correlation length R_c .

The parameters E_0 and σ were determined from the condition $r_c/R_c \rightarrow 0$ as $T \rightarrow T_c$ using Eq. (26) and the experimental phase diagram $T_c(x)$ for x above, but close to the critical concentration. As $T \rightarrow 0$, it follows from Eq. (26) that R_c/r_c approaches a maximum value $(1 - x/x_{cr})^{-1/2}$, which, if R_c/r_c is found to be approximately 2.6 from the fit, would correspond to $x/x_{cr} \approx 0.8$. The latter value is higher than the ratio of 0.5 expected for $x = 1\%$ and $x_{cr} \approx 2\%$. Part of the disagreement between theory and experiment can obviously be due to an uncertainty in the experimental value of x for this particular sample and of x_{cr} in general. The temperature

dependence of R_c/r_c calculated from Eq. (26) is represented in the inset of Fig. 3(a), where we have assumed that $x/x_{cr} \approx 0.8$. In this low-concentration sample, the presence of extrinsic random fields is also expected to introduce differences between theory and experiment. At low temperatures these fields will cause certain dipole configurations to be frozen. In this situation the correlation length R_c can be different for different parts of the sample, resulting, for $R_c^{-1} \lesssim q \lesssim r_c^{-1}$, in a more rapid decrease than that given in Eq. (17). Freezing of the dipoles at low temperatures also leads to disagreement between the values of R_c/r_c obtained from the Raman data and those one could expect from Eq. (13) using experimental values of ϵ/ϵ_0 (see Table I). The source of this disagreement lies in a long-time dielectric relaxation in KLT, that prevents the achievement of static equilibrium at low temperatures even for frequencies as low as 10^{-3} Hz .²⁰

In the present low-concentration sample, we did not observe a drop in the TO_2 line intensity, nor did we observe the appearance of a clear TO_3 line marking a long-range structural transition. This observation leads us to suggest that the drop in the TO_2 line intensity observed for higher concentrations is due to the appearance of large spontaneous strains associated with a structural transition that decrease the oxygen polarizability. This conclusion is also supported by the observation of a sevenfold or eightfold increase in the Bragg intensities associated with relief of extinction in the same samples.²¹ The further increase of the TO_2 line intensity at lower temperatures should then normally be attributed to an increase in the order parameter. We note, however, that no significant changes were noticed below T_c in the TO_2 line shape. This would suggest that the correlation length of the polarization R_c remains relatively constant below T_c .

ANALYSIS OF THE KTN SPECTRA

As shown by the results obtained for the TO_2 Raman line in KTN with 1.2%, 4%, and 15.7% Nb (see Figs. 1 and 3), the features of the line shape and linewidth in KTN are basically the same as in KLT. The TO_2 line is strongly asymmetric (broader on the high-frequency side), the width being smaller for KTN than for KLT. The linewidth decreases rapidly through the phase transition—the more rapid the decrease, the higher the concentration. It becomes constant below T_c and, in the case of the KTN with 1.2% Nb, is practically constant over the whole temperature range investigated.

One important difference between the two systems can be seen in the integrated intensity of the TO_2 line, which increases much more rapidly with decreasing temperature in KTN than in KLT. This observation can be understood if one recognizes that the reorientational frequencies of Nb ions in KTaO_3 are much higher than those for Li ions,²² but that there still exists a distribution of these frequencies. Within this distribution those Nb ions with $\nu < \Delta\omega_{\text{HM}}$ will contribute to the narrow TO_2 Raman line. The other Nb impurities, whose reorientation is faster, contribute only to the low-intensity, long

tail of the spectrum, which cannot be observed because of the background intensity. As the temperature decreases, more Nb ions satisfy the above condition, thus contributing to a faster increase of the integrated intensity. The previous explanation is supported by an investigation²³ of the first-order Raman line TO_1 corresponding to the soft mode in KTN with 1.2% Nb. These results indicated that the soft-mode frequency ω_s decreases with temperature above T_c , meaning that $\omega_s > \nu_{\text{Nb}}$.⁶ However, at $T_{\text{min}} \simeq 20$ K, ω_s reaches a minimum value of $\sim 1 \text{ cm}^{-1}$ and then increases again below 20 K. This undoubtedly suggests that, near T_{min} , $\omega_s \simeq \nu_{\text{Nb}}$. It should also be noted that we cannot attribute this "slowing down" of the Nb relaxation to critical effects since $T_c = 15$ K (Ref. 4) is significantly lower than T_{min} .

Let us now consider the 1.2% Nb case more quantitatively. As noted earlier for this concentration, the TO_2 linewidth is independent of temperature, and the line shape is the same as that for the slowly reorienting Li impurities, indicating that the reorientation frequencies of the contributing Nb ions are less than $\Delta\omega_{\text{HM}}$. We can thus write the integrated intensity as

$$I_N \sim \langle (P^\mu)^2 \rangle N(T), \quad (28)$$

where $\langle (P^\mu)^2 \rangle$ is given by Eq. (18) and $N(T)$ is the number of impurities with reorientational frequencies less than $\Delta\omega_{\text{HM}}$, i.e.,

$$N(T) = \int_0^{\Delta\omega_{\text{HM}}} \varphi(\nu) d\nu, \quad (29)$$

in which $\varphi(\nu)$ is the distribution function of these frequencies. To estimate $N(T)$ we take into account that, because of the random distribution of the impurity dipoles, there exist many close pairs with dipoles separated by less than the average distance $R = n^{-1/3}$ (n is the Nb concentration and $n = x/a^3$; a^3 is the lattice constant). The reorientation of the dipoles in such close pairs is slowed down because

$$\nu = \nu_0 e^{-U/T}, \quad (30)$$

where U is the potential acting on a given dipole from its close neighbors. In such a case, Eq. (29) can be rewritten as

$$N(T) = \int_{T \ln(\nu_0/\Delta\omega_{\text{HM}})}^{\infty} \varphi'(U) dU. \quad (31)$$

To calculate the distribution function $\varphi'(U)$, we use the form [Eq. (3.10) in Ref. 1]

$$U = A/r, \quad (32)$$

which is valid for highly polarizable crystals at $r < r_c$, where r is the distance between the two dipoles in the pair:

$$\begin{aligned} \varphi'(U) &= \left[\delta \left[U - \frac{A}{r} \right] \right] \\ &= 4\pi n \int dr r^2 \delta \left[U - \frac{A}{r} \right] e^{(-4\pi/3)nr^3}, \end{aligned} \quad (33)$$

where the distribution function for close neighbors has

been employed. Since the contributing Nb ions are those in "slow-relaxing" pairs for which $U > kT$, the greater T , the smaller is the r value that will contribute to (33). In order to obtain the first nonvanishing term at $T > T_c$, we can thus omit the exponent in Eq. (33). We finally obtain the following expression for the integrated intensity:

$$I_N \sim \langle (P^\mu)^2 \rangle \frac{1}{T^3}. \quad (34)$$

For $x_{\text{Nb}} \simeq 1.2\%$, Fig. 3(d) shows that this expression is in very good agreement with the experimental results.

For higher niobium concentrations (4% and 15.7% Nb), the calculated curve falls increasingly below the experimental one. This can be expressed differently by saying that, the higher the Nb concentration, the faster the TO_2 line intensity increases with decreasing temperature. This result is probably due to a stronger temperature dependence of $N(T)$ than $1/T^3$ in Eq. (34). For impurities separated by a lattice constant, interactions other than the dipolar type considered here may become important, and the long-wavelength limit used in Eq. (32) may no longer be valid. We also note that the factor $N(T)$ in Eq. (28) explains why the TO_2 integrated intensity is not found to be simply proportional to the Nb concentration.^{11,9}

CONCLUSION

We have reported experimental results for first-order Raman scattering from the polar TO_2 hard mode, both above and below the phase transition, in KLT and KTN. This first-order scattering can be attributed to the presence of polar microregions induced by the presence of Li or Nb impurities in the soft-mode system KTaO_3 . These Raman results can be reasonably explained by a theory that takes into account the special form (dispersion) of the polar fluctuations induced by randomly distributed, interacting off-center ions in highly polarizable crystals. In particular, the theory properly describes the characteristic asymmetry of the TO_2 Raman line and its integrated intensity. For the latter the agreement between theory and experiment could be improved by taking into account, for the KLT case, a dynamical contribution and, for both KLT and KTN at higher concentrations, many-body interactions beyond dipolar-pair interactions. The most important parameter obtained from the fit of the TO_2 spectra is the ratio of the polarization correlation lengths r_c and R_c , respectively, for the pure and doped systems. One can see that, close to T_c , R_c is relatively small when compared to the domain sizes in normal ferroelectrics. Even at low temperatures, R_c does not appear to grow to very large values—as evidenced by the persistence of the TO_2 line asymmetry. Comparing the line shape observed for KLT and KTN for different concentrations, we conclude that R_c is smaller in KLT, but that it does not seem to vary significantly with the concentration of impurities. A secondary parameter obtained from the theoretical analysis of the experimental data is ν_h/r_c , which shows a reasonable correlation with the soft-mode frequency obtained from the position of the TO_1 line. The present analysis also explains why the in-

tegrated TO_2 line intensity grows faster with decreasing temperature in KTN than in KLT. This explanation rests on the dynamical character of a large number of off-center Nb ions at high temperature and suggests that the minimum observed in the soft- TO_1 -mode frequency²¹ corresponds to a transition to the static regime $\nu < \omega_s$. For higher concentration one should also take into consideration the effect of the critical slowing down of the Nb fluctuations based on Eqs. (19)–(21). This analysis will be reported elsewhere.

We finally note that first-order Raman scattering accompanying a central peak above T_c has also been ob-

served in other systems such as cubic KMnF_3 and RbCaF_3 .¹⁰

ACKNOWLEDGMENTS

This work was partially supported by the Office of Naval Research Grant No. N00014-90-J-4098 (Lehigh) and by the Division of Materials Sciences, U.S. Department of Energy, under Contract No. DE-RC05-84OR21400 (Oak Ridge) with the Martin Marietta Energy Systems, Inc. We owe particular thanks to K. B. Lyons and D. Rytz for making the 1.2% crystal available to us.

-
- ¹B. E. Vugmeister and M. D. Glinchuk, *Rev. Mod. Phys.* **62**, 938 (1990).
²U. T. Hochli, K. Knorr, and A. Loidl, *Adv. Phys.* **39**, 405 (1990).
³W. Kleemann, S. Kutz, F. J. Schafer, and D. Rytz, *Phys. Rev. B* **37**, 5856 (1988).
⁴J. Toulouse, P. DiAntonio, B. E. Vugmeister, X. M. Wang, and L. A. Knauss, *Phys. Rev. Lett.* **68**, 232 (1992).
⁵C. A. Azzini, C. P. Banfi, G. Giolotto, and U. T. Hochli, *Phys. Rev. B* **43**, 7473 (1991).
⁶B. I. Halperin and C. M. Varma, *Phys. Rev. B* **14**, 4030 (1976).
⁷B. E. Vugmeister and M. D. Glinchuk, *Zh. Eksp. Teor. Fiz.* **79**, 947 (1980) [*Sov. Phys. JETP* **52**, 482 (1980)].
⁸Y. Yacoby, *Z. Phys. B* **31**, 275 (1978).
⁹H. Uwe, K. B. Lyons, H. L. Carter, and P. A. Fleury, *Phys. Rev. B* **33**, 6436 (1986).
¹⁰A. D. Bruce, W. Taylor, and A. F. Murray, *J. Phys. C* **13**, 483 (1980).
¹¹R. L. Prater, L. L. Chase, and L. A. Boatner, *Phys. Rev. B* **23**, 221 (1981).
¹²S. K. Manliet and H. Y. Fan, *Phys. Rev. B* **5**, 4046 (1972).
¹³B. E. Vugmeister, *Fiz. Tverd. Tela (Leningrad)* **26**, 1080 (1984) [*Sov. Phys. Solid State* **26**, 658 (1984)].
¹⁴Y. Yacoby, *Z. Phys. B* **41**, 269 (1981).
¹⁵B. E. Vugmeister, *Fiz. Tverd. Tela (Leningrad)* **27**, 1190 (1985) [*Sov. Phys. Solid State* **27**, 716 (1985)].
¹⁶U. T. Hochli, H. E. Weibel, and L. A. Boatner, *Phys. Rev. Lett.* **41**, 1410 (1978).
¹⁷P. Doussineau, J. Toulouse, K. McEnaney, C. Fresnois, and A. Levelut, *Europhys. Lett.* (to be published).
¹⁸B. E. Vugmeister and V. A. Stefanovich, *Zh. Eksp. Teor. Fiz.* **97**, 1867 (1990) [*Sov. Phys. JETP* **70**, 1053 (1990)].
¹⁹B. E. Vugmeister, *Ferroelectrics* **120**, 133 (1991).
²⁰F. Wickenhofer, W. Kleemann, and D. Rytz, *Ferroelectrics* **124**, 237 (1991).
²¹J. Toulouse and B. Hennion (unpublished).
²²G. Samara, *Phys. Rev. Lett.* **53**, 298 (1984).
²³H. Chou, S. M. Shapiro, K. B. Lyons, J. Kjems, and D. Rytz, *Phys. Rev. B* **41**, 7231 (1990).